ARTICLE IN PRESS

Renewable Energy xxx (2016) 1–12

Contents lists available at ScienceDirect

Renewable Energy

journal homepage: www.elsevier.com/locate/renene

Optimal design of synergistic distributed renewable fuel and power systems

Andrew Allman, Prodromos Daoutidis*

Department of Chemical Engineering and Materials Science, University of Minnesota, Minneapolis, MN 55455, USA

A R T I C L E I N F O

Article history:
Received 29 January 2016
Received in revised form
10 March 2016
Accepted 14 March 2016
Available online xxx

Keywords:
Renewable energy
Optimization
Microgrid
Biorefinery
Distributed energy systems
System of systems

A B S T R A C T

The concepts of the biorefinery and microgrid have emerged as ways to increase the sustainability of the energy infrastructure. Although typically considered as separate systems, synergies exist between the biorefinery and the microgrid, suggesting that a combined system could be more efficient than the individual systems. This paper explores this hypothesis by comparing the optimal designs and costs of the individual, and the combined biorefinery and microgrid systems. A novel design optimization problem considering synergistic operation of the biorefinery and microgrid is presented. A solution method to this problem is developed that exploits the separable nature of the optimization of such a "system of systems." Base case results show that the combined system costs are higher than those of the individual systems. However, by implementing a hydrogen recycle, significant savings are seen in the combined system, highlighting a direct advantage of system synergy. The effects of energy autonomy on the system are also analyzed and discussed. The overall analysis shows that the synergies between the biorefinery and microgrid can be exploited to create an energy system that is less costly and more efficient than the sum of its constituent parts.

1. Introduction

The current energy landscape is evolving due to concerns about anthropogenic climate change, sustainability, cybersecurity, and aging infrastructure. As this change occurs it is essential to develop new systems that promote the usage of local renewable resources, protect users against major outages in energy supply, and respond to local energy demands. Distributed renewable fuel and power systems offer many potential advantages to this end [1–3]. Such systems can be placed close to end users and operate with minimal demand from the centralized energy infrastructure.

Individually, renewable power and fuel systems have been extensively researched in the context of the microgrid and the biorefinery, respectively. The microgrid is a small scale power system that allows for high penetration of renewable resources and dispatchable fossil fuel power generators. Such a system is particularly useful for primary power of islands and rural areas, or as backup power for critical infrastructure in larger communities. Various studies exist that have explored the problem of microgrid optimal design. The optimal design of wind and solar power generation system with hydrogen storage is examined in Ref. [4]. Ref. [5] performs a multi-objective optimization for the design of an isolated power system utilizing wind, solar, hydrogen, diesel, and batteries. The effects of using a diesel microturbine combined with renewables, as well as the effect of grid-connection, is analyzed in Ref. [6]. Ref. [7] examines more closely the effect of location on microgrid optimal design. The polygeneration of power and chemicals has also been studied, mainly in the context of methanol production in conjunction with gasification of coal or biomass [8,9]. Missing in the literature are studies that model an entire renewable microgrid operating in synergy with a large-scale fuel production plant, such as a biorefinery, so as to meet the entire energy needs of a community.

The biorefinery exists as a parallel to oil refineries, producing essential fuels and chemicals using a biomass, rather than crude oil, feedstock. Biorefineries are poised to play an increasingly important role in the chemical infrastructure as technology improves and sustainability concerns become more important. Various studies have also explored optimal design of biorefineries. Ref. [10] uses superstructure based optimization to analyze the tradeoffs between the production of fuels and commodity chemicals in a biorefinery. Refs. [11] and [12] perform an in-depth modeling and

* Corresponding author.
E-mail address: daout001@umn.edu (P. Daoutidis).

http://dx.doi.org/10.1016/j.renene.2016.03.051
0960-1481/

Please cite this article in press as: A. Allman, P. Daoutidis, Optimal design of synergistic distributed renewable fuel and power systems, Renewable Energy (2016), http://dx.doi.org/10.1016/j.renene.2016.03.051

Nomenclature

Sets

$a \in \{1,\ldots,4\}$ Atoms
$f \in \{1,\ldots,4\}$ *Feedstocks*
$i \in \{1,\ldots,I\}$ Mass streams
$j \in \{1,\ldots,J\}$ Energy streams
$k \in \{1,\ldots,23\}$ Mass components
$r \in \{1,\ldots,10\}$ Reactors
$u \in \{1,\ldots,U\}$ Microgrid Units
$t \in \{1,\ldots,8760\}$ Hours in a year

Variables

$a_{a,i}$	Mass fraction of atom a in stream i
$\dot{e}_{j,t}$	Energy flowrate for stream j at time t
f_f	Fraction of feed with feedstock f
F	Fuel shared from biorefinery to microgrid
h_t	mount of hydrogen stored at time t
H	Hydrogen shared from microgrid to biorefinery
$\lambda_{a,r}$	Lagrange multipliers in equilibrium reactor r for atom a
$\dot{m}_i$	Mass flowrate for stream i
q_r	Heat requirements for reactor r
q_i	Preheat requirements for stream i
Q	Heat shared from microgrid to biorefinery
V_t	Fuel stored at time t
$x_{i,k}$	Mass fraction of component k in stream i
$y_{u,t}$	Binary variable representing on/off state of unit u at time t
z_u	Microgrid unit capacities

Parameters

$\alpha_{a,k}$	Atomic fraction of atom a in component k
γ_r	Capacity exponent for reactor r
δ_f	Fuel demand
$\delta_{h,t}$	Heat demand at time t
$\delta_{p,t}$	Fuel demand at time
$\Delta H_{f,k}$	Specific heat of formation of component k
η_u	Efficiency of unit u
ζ_f	Cost of feedstock f
ζ_{fuel}	Cost of fuel
ζ_h	Cost of heat
ζ_{H_2}	Cost of hydrogen
ζ_u	Relative operating cost of unit u
Θ	Scaled number of years for NPV formulation
ξ_r	Reference capital cost of reactor r
ξ_u	Relative capital cost of unit u
ρ	Fraction of hydrogen recycled
$\phi_{f,k}$	Fraction of component k in feedstock f
χ_r	Reference capacity of reactor r
$\psi_{k,r}$	Yield of component k in reactor r
ω	Fraction of autonomy of system
A,B,C,D,E	Heat capacity equation coefficients
$c_{p,k}$	Heat capacity of component k
E_t	Solar irradiance at time t
M	Big-M formulation upper bound
T_r	Operating temperature of a reactor r
v_t	Wind speed at time t
v_{ci}	Wind turbine cut-in speed
v_{co}	Wind turbine cut-out speed
v_r	Wind turbine rated speed

optimization study to find the optimal design of a biomass to liquid fuels plant. Ref. [13] used an automated targeting approach to identify biorefinery pathways to maximize revenue. In Ref. [14], tree graphs are used in a "forward–backward" approach to match biomass feedstocks and products with conversion technologies. Ref. [15] performs a superstructure optimization under both economic and environmental objective considerations for a gasification-based biorefinery.

While both the biorefinery and the microgrid help to promote renewable energy sources, these systems by themselves cannot operate without reliance on the centralized infrastructure. Microgrids typically rely on an externally obtained fuel or connection to the macrogrid when renewables are not readily available, while biorefineries require utilities for the chemical processes to run. As such, these systems cannot be truly resilient to potential issues in the centralized infrastructure. However, when considered together, the two systems each have outputs that satisfy the needs of the other as shown in Fig. 1. By taking advantage of these synergies, it is hypothesized that a combined biorefinery and microgrid system can meet local energy demands at lower cost and with less demand on the centralized infrastructure than the systems can individually.

This paper presents a first of its kind design optimization study of a combined biorefinery and microgrid system. The objective of the paper is to compare the costs and designs of a combined system to those of the individually optimized systems. Section 2 presents the mathematical models for the individual and combined systems. Section 3 presents the results of solving these optimization models and discussion of a case study of the proposed system using data from Minneapolis, MN. Cases where hydrogen is recycled within the biorefinery and where the autonomy of the energy system is varied are analyzed and discussed in addition to the base case. Lastly, section 4 presents some concluding remarks and discusses future directions of this research.

2. Problem formulation

2.1. Biorefinery

The biorefinery superstructure utilizes many of the technologies

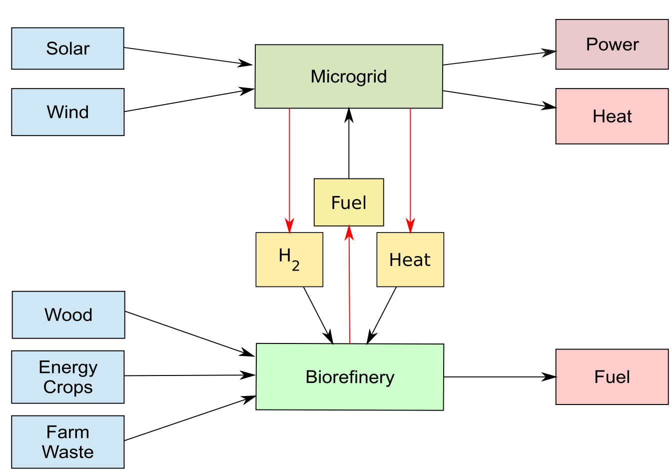

Fig. 1. High-level depiction of proposed system of systems, highlighting synergies with red arrows. (For interpretation of the references to color in this figure legend, the reader is referred to the web version of this article.)

Please cite this article in press as: A. Allman, P. Daoutidis, Optimal design of synergistic distributed renewable fuel and power systems, Renewable Energy (2016), http://dx.doi.org/10.1016/j.renene.2016.03.051

considered in Refs. [10] and [12], but considers only the production of liquid fuels. Fig. 2 shows the superstructure with all considered conversion technologies. The optimization program will decide which technologies to use to meet fuel demand. The optimization will also decide which biomass feedstock to use between switchgrass, corn stover, wheat straw, and poplar wood chips. The candidate feedstocks were chosen since they do not compete with the food supply.

Biomass fed into the system can either be sent to a biofine reactor or directly to a gasifier. The biofine process fractionates lignocellulose via acid catalyzed hydrolysis and reactions that result in cellulose conversion to levulinic acid (LA) and hemicellulose conversion to furfural [16]. LA is converted to liquid fuel via a three step process, first dehydrating LA to γ-valerolactone (GVL), then decarboxylating GVL to butene, and finally oligomerizing butene to liquid hydrocarbons [17]. Furfural is converted to liquid fuel via a two step process, first hydrogenating furfural to 2-methyl furan (2MF) and lastly further hydrogenating MF to diesel-range hydrocarbons [18]. The leftover lignin, char, and tars can be sent to a gasifier for further processing or simply outputted as waste. Gasified biomass must be shifted to a proper hydrogen to carbon dioxide molar ratio of 2 for further processing. This analysis considers adding hydrogen rather than performing a water gas shift reaction, since hydrogen could in theory be obtained from the microgrid system when considering synergistic operation. This limits the carbon dioxide emissions that would result from a traditional water–gas shift reactor. Shifted syngas can be used to generate gasoline-range hydrocarbons using either a Fischer–Tropsch synthesis or a methanol synthesis and upgrading pathway [12]. As a first step, the model assumes perfect separations to separate components after each reactor.

An optimization problem was formulated to decide how to best design this biorefinery to meet fuel demand at minimal cost. A 20-year net present value (NPV) cost is used, assuming a 7% discount rate:

$$\text{minimize} \sum_r \left(\xi_r \left(\frac{\dot{m}_{in}}{\chi_r} \right)^{\gamma_r} \right) + 8760\Theta \left(\dot{m}_1 \sum_f \zeta_f f_f + \zeta_{H_2} \sum_{i \in H_2 \text{ feeds}} \dot{m}_i + \zeta_h \left(\sum_r q_r + \sum_i q_i \right) \right) \tag{1}$$

In equation (1), capital costs are nonlinear due to economies of scale in building chemical reactors. Hourly operating costs include the costs of purchasing feedstock and utilities, and are multiplied by the number of hours in a year and the scaled number of years due to the NPV formulation. Costs of 7¢/kWh heat and \$1/kg H_2 are assumed. Table 1 lists the parameters used for reactor capital cost calculation. Costs from older references are adjusted for inflation assuming 3% inflation per year.

The optimization is constrained such that a specified fuel demand must be met:

$$\sum_{i \in \text{fuel outputs}} \dot{m}_i = \delta_f \tag{2}$$

Additional constraints consist of mass and energy balances throughout the system. In every reactor and at every split point the total mass balance must hold:

$$\sum_{i \in inlets} \dot{m}_i = \sum_{i \in outlets} \dot{m}_i \tag{3}$$

Additionally, atomic mass balances hold at every reactor and split point:

$$\sum_{i \in inlets} a_{a,i} \dot{m}_i = \sum_{i \in outlets} a_{a,i} \dot{m}_i \ \forall a \tag{4}$$

Atomic mass fractions are determined from component mass fractions:

$$a_{a,i} = \sum_k \alpha_{a,k} x_{i,k} \ \forall a, i \tag{5}$$

Carbon, oxygen, and hydrogen are considered as the key elements to keep track of. The remaining trace elements are lumped into a generic "ash" atom and are assumed not to react. Mass fractions, both atomic, component, and feed, must add to one:

$$\sum_k x_{i,k} = 1 \ \forall i \tag{6}$$

$$\sum_a a_{a,i} = 1 \ \forall i \tag{7}$$

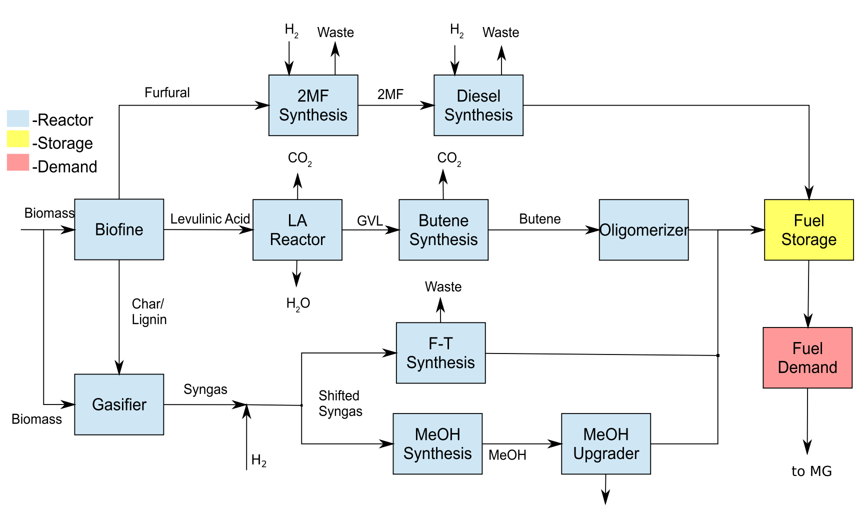

Fig. 2. Superstructure considered for biorefinery system.

Please cite this article in press as: A. Allman, P. Daoutidis, Optimal design of synergistic distributed renewable fuel and power systems, Renewable Energy (2016), http://dx.doi.org/10.1016/j.renene.2016.03.051

Table 1
Reactor capital cost parameters for use in equation (1).

Reactor	Reference Cost	Reference Capacity	Scaling Exponent	Ref
Pretreatment	$27.0 MM	83,333 kg/hr	0.67	[19]
Biofine	$196.0 MM	41,667 kg/hr	0.6	[16]
Gasifier	$170.4 MM	180,833 kg/hr	0.67	[11]
2MF + Diesel Synthesis	$65.0 MM	104,167 kg/hr	0.6	[20]
LA Reactor	$5.8 MM	5140 kg/hr	0.6	[17]
Butene Synthesis	$4.5 MM	3110 kg/hr	0.6	[17]
Oligomerizer	$3.2 MM	1730 kg/hr	0.6	[17]
F–T Synthesis	$765 MM	958,333 kg/hr	0.67	[21]
MeOH Synthesis	$15.3 MM	129,167 kg/hr	0.6	[22]
MeOH Upgrader	$21.6 MM	38,333 kg/hr	0.6	[22]

$$\sum_f f_f = 1 \tag{8}$$

Biomass initially consists of cellulose, hemicellulose, lignin, and char at various compositions depending on the feedstock [23]. Data for each feedstock considered is shown in Table 2. Initial mass fractions are determined from the feedstocks chosen:

$$x_{1,k} = \sum_f \phi_{f,k} f_f \;\; \forall k \tag{9}$$

The majority of reactors in the system are modeled as yield-based. This means that the mass flowrate of a component exiting a reactor can be determined by the mass flowrate of a key component entering the reactor:

$$x_{out,k}\dot{m}_{out} = \psi_{r,k} x_{in,key}\dot{m}_{in} \tag{10}$$

Table 3 displays the yields of the reactors in the system. Hydrogen inputs required for certain reactors and outputs of components such as carbon dioxide and water are determined using stoichiometry.

For the gasifier and methanol synthesis reactors, using a simple yield based reactor will not give accurate results. Instead, chemical equilibrium is used to model each of these reactors. Chemical equilibrium occurs when the Gibbs free energy (G) of a system is minimized, which leads to the following optimization subproblem [25]:

$$\begin{aligned} &\text{minimize } G(x_{out,k}) \\ &\text{s.t.} \sum_{i \in inlets} a_{a,i}\dot{m}_i = \sum_{i \in outlets} a_{a,i}\dot{m}_i \;\; \forall a \end{aligned} \tag{11}$$

Formulation [11], however, cannot be placed into the overall optimization problem as written. To this end, the equilibrium subproblem is reformulated using the Lagrangian ($\mathscr{L}$) formulation:

Table 3
Reactor yields for major products.

Reactor	Key Input	Output	Yield	Ref
Biofine	Cellulose	LA	50.0%	[16]
	Cellulose	Formic acid	19.9%	[16]
	Cellulose	Char	30.1%	[16]
	Hemicellulose	Furfural	50.1%	[16]
	Hemicellulose	Char	49.9%	[16]
2MF Synthesis	Furfural	2MF	74.3%	[18]
	Furfural	Waste organics	12.7%	[18]
Diesel Synthesis	2MF	Diesel	75.0%	[18]
	2MF	Light gas	1.95%	[18]
	2MF	Middle hydrocarbons	1.76%	[18]
LA	LA	GVL	61.7%	[17]
Butene Synthesis	GVL	Butene	55.4%	[17]
Oligomerizer	Butene	C_8	29.7%	[17]
	Butene	C_{12}	25.7%	[17]
	Butene	C_{16}	24.8%	[17]
	Butene	C_{20}	18.8%	[17]
FT Synthesis	Carbon monoxide	F-T gasoline	22.6%	[24]
	Carbon monoxide	Light gas	11.3%	[24]
MeOH Upgrading	Methanol	Gasoline	45.9%	[22]
	Methanol	Light gases	5.6%	[22]

$$\mathscr{L}(x_{out,k}, \lambda_{a,r}) = G(x_{out,k}) + \sum_a \lambda_{a,r}\left(\sum_{i \in inlets} a_{a,i}\dot{m}_i - \sum_{i \in outlets} a_{a,i}\dot{m}_i\right) \tag{12}$$

$$\nabla(\mathscr{L}) = 0 \tag{13}$$

An advantage of using Gibbs free energy minimization to model equilibrium is that individual equilibrium reactions need not be specified, only species that will be present in the output at a non-negligible amount. For the gasifier, these include CO, CO_2, H_2O, H_2, and char. For the methanol synthesis reactor, these include CO, CO_2, H_2O, H_2, and methanol.

Energy balances are required to keep track of heat requirements through the system. It is necessary to consider reactor preheating and heat management inside the reactor. For heat management in a reactor, isothermal operation is assumed. It is also assumed that the cost of cooling is negligible, such that only positive values of heat

Table 2
Biomass data.

Feedstock	% Cellulose	% Hemicellulose	% Lignin	% C	% H	% O	Cost (¢/kg)
Corn Stover	36.20	23.23	18.50	47.04	5.47	36.51	5.0
Wheat Straw	33.47	23.20	17.28	43.88	5.26	39.85	5.0
Wood Chips	43.91	20.76	27.29	49.37	5.75	42.31	5.5
Switchgrass	31.39	24.72	18.00	47.27	5.31	41.05	6.6

demand are recorded. As such, the heat demand is that which maintains isothermal operation:

$$q_r = \max\left(0, \sum_{i\in outlets}\sum_k x_{i,k}\dot{m}_i \Delta H_{f,k}(T_r) - \sum_{i\in inlets} \times \sum_k x_{i,k}\dot{m}_i \Delta H_{f,k}(T_r)\right) \tag{14}$$

The heat of formation is a function of temperature and is determined as follows:

$$\Delta H_{f,k}(T_r) = \Delta H_{f,k}(298K) + \int_{298K}^{T_r} c_{p,k}(T)dT \tag{15}$$

For solids and liquids, heat capacity is assumed to be constant with respect to temperature. This is a poor assumption for gases, whose heat capacity varies with temperature as follows:

$$c_{p,k}(T) = A + BT + CT^2 + DT^3 + ET^{-2} \tag{16}$$

Heats of formation at 298 K and parameters for equation (16) are obtained using [26]. For energy required for preheating, it is assumed that no temperature changes occur such that the reactor temperatures can be used as the in and out temperatures of the preheater:

$$q_i = \max\left(0, \sum_k \left(x_{i,k}\dot{m}_i \int_{T_{in}}^{T_{out}} c_{p,k}(T)dT\right)\right) \tag{17}$$

Lastly, all variables are nonnegative quantities. Equations (1–17) specify the optimization problem for the biorefinery. This problem is a nonlinear program due to various bilinear terms and nonlinear equilibrium and capital cost terms. It can be solved using the BARON solver in GAMS, but good bounds are required to ensure global optimality [27]. Bounds were determined by solving the biorefinery mass balance at various extreme cases, for example using only corn feedstock, directed through only gasification and Fischer–Tropsch synthesis, or using only grass feedstock directed through the biofine pathway. This is implemented by fixing feed fractions to 1 and flowrates to zero, allowing for the general mass balances to hold without the introduction of integer variables, which would increase the problem complexity. The final optimization problem consists of 702 variables and 243 equations.

2.2. Microgrid

The microgrid superstructure utilizes most of the technologies used in Ref. [28]. However, a hydrogen system utilizing an electrolyzer and fuel cell is used for energy storage instead of a battery, in anticipation of hydrogen produced being used in the biorefinery. Fig. 3 shows the microgrid superstructure with all considered energy technologies. The optimization program will decide the capacities of all units within the microgrid, as well as operating points for the electrolyzer, fuel cell, electric heater, and microturbines at each time point.

An optimization problem was formulated to decide how best to design this microgrid to meet heat and power demand at minimal cost. Again, a 20-year NPV cost formulation at a 7% discount rate is used to quantify cost. The objective function is thus as follows:

$$\text{minimize } \sum_u \xi_u z_u + \Theta\left(\sum_t\left(\sum_u \zeta_u \dot{e}_{in,t} + \zeta_{fuel}\dot{e}_{fuel,t}\right)\right) \tag{18}$$

Cost data for microgrid units is shown in Table 4. It is assumed that diesel fuel is used and purchased at $3/gal.

The first constraint for this problem is that heat and power demand is met at each hour throughout the year:

$$\sum_{j\in \text{power out}} \dot{e}_{j,t} = \delta_{p,t} \ \forall t \tag{19}$$

$$\sum_{j\in \text{heat out}} \dot{e}_{j,t} \geq \delta_{h,t} \ \forall t \tag{20}$$

Data for heat demand, power demand, as well as solar irradiance and wind speed is available at hourly time points throughout a typical meteorological year for many locations [33]. Heat output is allowed to exceed demand if necessary due to excess heat from microturbines, with excess heat being applied to cooling water at negligible cost. The optimization problem is further constrained by various physical requirements. First, the energy balance must also hold at all points where energy streams meet or split:

$$\sum_{j\in \text{inlets}} \dot{e}_{j,t} = \sum_{j\in \text{outlets}} \dot{e}_{j,t} \ \forall t \tag{21}$$

Each microgrid unit takes in a certain type of energy or mass flow and outputs a different kind of energy or mass flow. A thermodynamic efficiency is used for each unit:

$$\dot{e}_{out,t} = \eta_u \dot{e}_{in,t} \ \forall u,t \tag{22}$$

Since hydrogen is the main energy storage in the microgrid system, hydrogen flows from the electrolyzer and to the fuel cell are considered to be energy flows for the sake of analysis. Table 5 lists the efficiencies of the units in the microgrid. The wind turbine, however, is not modeled using equation (22). To obtain a more accurate description of wind power, the following equation is used:

$$\dot{e}_{wind,t}(v_t) = \begin{cases} 0, & v_t \leq v_{ci}, v_t \geq v_{co} \\ z_{wind}\dfrac{v_t^3 - v_{ci}^3}{v_r^3 - v_{ci}^3}, & v_{ci} < v_t \leq v_r \\ z_{wind}, & v_r < v_t < v_{co} \end{cases} \tag{23}$$

Solar data from Ref. [33] is given in irradiance. To convert this to an energy flow, the data must be multiplied by the area of solar panels:

$$\dot{e}_{sun,t} = z_{solar}E_t \ \forall t \tag{24}$$

Fuel flow to the microturbine is tracked in terms of the higher heating value (HHV) of the fuel. Output power from the microturbine must be less than the microturbine rating:

$$\dot{e}_{\text{MT power out},t} \leq z_{MT} \ \forall t \tag{25}$$

Hydrogen is produced in the electrolyzer and sent to a storage tank. Binary variables are used to keep track of the on-off states of the electrolyzer and fuel cell. The two units cannot be running at the same time:

$$y_{el,t} + y_{fc,t} \leq 1 \ \forall t \tag{26}$$

The model does not consider any penalty terms for cycling units on and off. Big-M formulation [37] is used to ensure no flow occurs out of a unit when it is off:

$$\dot{e}_{out,t} \leq My_{u,t} \ \forall u,t \tag{27}$$

It is also essential to keep track of the amount of hydrogen stored at each time point, which is done through the following

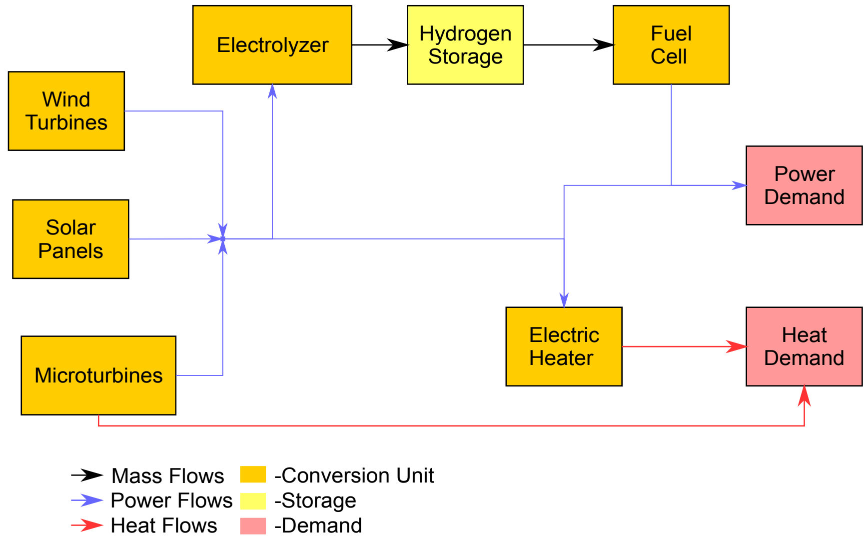

Fig. 3. Superstructure considered for microgrid system.

Table 4
Cost data for microgrid units.

Unit	Capital Cost	Operating Cost	Ref
Wind Turbine	\$2500/kW	0.8¢/kWh	[28,29]
Solar Panel	\$6100/kW	\$52/kW installed/yr	[28,30]
Microturbine	\$3600/kWe	2¢/kWh	[28]
Electrolyzer	\$25,050/(kg H_2/hr) flowrate	6¢/kWh	[31]
Fuel Cell	\$3000/kW	6¢/kWh	[32]
Electric Heater	\$60/kW	0.75¢/kWh	[28]

Table 5
Conversion efficiencies in microgrid.

Conversion Unit	Input	Output	Efficiency	Ref
Solar Panel	kW solar irradiance	kW power	0.15	[34]
Microturbine	kW fuel HHV	kW power	0.23	[28]
Microturbine	kW fuel HHV	kW heat	0.46	[28]
Electrolyzer	kW power	kg/hr H_2	0.021	[35]
Fuel Cell	kg/hr H_2	kW power	16.5	[36]
Electric Heater	kW power HHV	kW heat	1	[28]

discretized dynamic mass balance of the hydrogen storage tank:

$$h_t = h_{t-1} + \dot{e}_{in,t-1} - \dot{e}_{out,t-1} \ \forall t \tag{28}$$

Electrolyzer, fuel cell, and heater unit capacities must be large enough to accommodate all possible energy inputs throughout the year:

$$z_u \geq \dot{e}_{in,t} \ \forall u, t \tag{29}$$

Similarly, the hydrogen tank size must be sufficiently large enough to accommodate all possible levels of hydrogen storage:

$$h_{max} \geq h_t \ \forall t \tag{30}$$

In practice, equations (29) and (30) determine the capacity of the microgrid units by finding the largest energy flow or storage within those units during all time points considered.

Lastly, all variables are nonnegative quantities. Equations (18–30) denote the optimization problem for the microgrid. This optimization problem is a mixed integer linear program (MILP) which can be solved using the CPLEX solver in GAMS. The final optimization problem consists of 61,330 variables and 96,361 equations. The large number of variables and constraints is due to the fact that unlike the biorefinery, microgrid operation is time dependent, therefore different variables must exist and constraints must hold for all 8760 h in the year. Despite the orders of magnitude increase in problem size with respect to the biorefinery, the linearity of the microgrid problem allows it to be solved with relative ease.

2.3. Combined system

The previous two subsections define the individual biorefinery and microgrid systems. Each optimization problem can be solved separately to find minimum cost designs that allow the biorefinery to meet fuel demand and the microgrid to meet heat and power demand, without any interactions between the two systems. To optimize the systems together, the following objective function is considered:

$$\text{minimize} \sum_u \xi_u z_u + \sum_r \xi_r \left(\frac{(\dot{m}_{in})}{\chi_r}\right)^{\gamma_r} + \Theta\left(8760\dot{m}_1 \sum_f \zeta_f f_f + \sum_u \sum_t \zeta_u \dot{e}_{in,t}\right) \tag{31}$$

Equation (31) is a sum of the objectives from the microgrid and biorefinery that neglects the purchasing costs of fuel, hydrogen, and heat utility, as these are now obtained within the combined system instead of purchased from elsewhere. All of the constraints that govern the physical systems defined in the previous two sections are used in the combined system, with the following additions and modifications.

First, hydrogen demand in the biorefinery is met by the microgrid. To enforce this, the dynamic hydrogen mass balance is modified to track an additional output, H, from the storage tank:

$$h_t = h_{t-1} + \dot{e}_{in,t-1} - \dot{e}_{out,t-1} - H \ \forall t \tag{32}$$

An equation is added defining H as the net hydrogen demand of the biorefinery:

Please cite this article in press as: A. Allman, P. Daoutidis, Optimal design of synergistic distributed renewable fuel and power systems, Renewable Energy (2016), http://dx.doi.org/10.1016/j.renene.2016.03.051

$$H = \sum_{i \in H_2 \text{ feeds}} \dot{m}_i \tag{33}$$

The fuel produced from the biorefinery needs to now not only meet the local fuel demand but also the demand of the microturbines. Thus, equation (2) is modified to:

$$\sum_{I \in \text{fuel outputs}} \dot{m}_i = \delta_f + F \tag{34}$$

The fuel passed to the microgrid does not need to be used right away but can instead be stored. Thus, a dynamic fuel mass balance is required, analogous to that for hydrogen storage:

$$V_t = V_{t-1} + F - \dot{e}_{fuel,t-1} \ \forall t \tag{35}$$

Lastly, heat production must be increased to meet the utility requirement of the biorefinery. Thus, equation (20) is modified to:

$$\sum_{j \in \text{heat out}} \dot{e}_{j,t} \geq \delta_{h,t} + Q \ \forall t \tag{36}$$

Again, an equation is added defining Q as the net heat demand of the biorefinery:

$$Q = \sum_r q_r + \sum_i q_i \tag{37}$$

Overall, the combined system optimization is a mixed integer nonlinear program (MINLP), which can in theory be solved by the BARON solver in GAMS. However, the model consists of 62,302 variables and 96,604 equations. Because the combined system optimization problem retains the nonlinear character of the biorefinery and the large number of variables and equations from the microgrid, it cannot be solved without additional reformulation.

To transform the combined optimization into a more tractable formulation, a primal decomposition is used [38]. To utilize primal decomposition, the optimization problem must be in the following form:

$$\begin{aligned} \text{minimize } & f(x,y,z) = f_1(x,z) + f_2(y,z) \\ \text{s.t } & F_1(x,z) = 0 \\ & F_2(y,z) = 0 \end{aligned} \tag{38}$$

The structure presented in equation (38) corresponds naturally to an optimization problem for a combined system of two subsystems, where x, f_1, and F_1 are the variables, objective, and constraints from subsystem 1, y, f_2, and F_2 are the variables, objective, and constraints from subsystem 2, and z are variables shared between the two subsystems. In the case being considered here, subsystem 1 would be the biorefinery, subsystem 2 would be the microgrid, and the shared variables would be the heat, hydrogen, and fuel shared between the two systems. When an optimization problem takes the form of equation (38), the following is an equivalent representation:

$$\begin{aligned} & \text{minimize } \varphi_1(z) + \varphi_2(z) \\ \text{s.t. } & \varphi_1(z) = \min_x (f_1(x,\zeta) | F_1(x,\zeta) = 0, \zeta = z) \\ & \varphi_2(z) = \min_y (f_2(y,\zeta) | F_2(y,\zeta) = 0, \zeta = z) \end{aligned} \tag{39}$$

In this case, equation (39) shows that the combined system can be optimized in a two step process. First, the individual biorefinery and microgrid subsystems are minimized at fixed values of shared heat, hydrogen, and fuel. Then, the combined system is optimized with respect to the shared variables.

This problem is still a challenging task since two optimization subproblems need to be solved as three different variables vary. Since these subproblems are not convex, algorithms such as gradient descent cannot be used to intelligently vary the shared variables to converge to a guaranteed global optimum. However, heat and hydrogen demands are largely dependent on the biorefinery pathway chosen, making shared fuel the key decision variable connecting the two subsystems. The algorithm depicted in Fig. 4 and described below was used to take advantage of this fact to find a solution more efficiently. First, a range of feasible values and step size for the amount of fuel shared in the combined system is defined. The algorithm then iterates through each shared fuel value. At each iteration, the biorefinery is solved allowing purchases of heat and hydrogen from outside sources. To ensure that all pathways are considered, the biorefinery is solved twice: with and without a constraint requiring the use of biofine hydrolysis (the reason for which will become apparent in the case study results). After each biorefinery solution, hydrogen and heat purchases are stored as the shared variables and the microgrid is solved. The biorefinery and microgrid costs, minus the biorefinery purchasing costs of hydrogen and heat, are then added. The minimal total cost of the two optimizations is stored for each shared fuel value. The combined system optimal design is obtained after stepping through all discrete values of shared fuel and selecting the minimum cost from all optimizations.

The above algorithm does not guarantee a global optimum since discrete steps are being used for a variable, and only one, instead of all three, of the shared variables are being completely varied. However, it does guarantee a feasible, near-optimal design point while also allowing different shared fuel iterations to be run in parallel. This point can then be compared with a lower bound on the optimal value, which is obtained by taking convex relaxations of the combined problem. To this end, bilinear terms are relaxed using McCormick relaxations [39]. Nonlinear and nonconvex

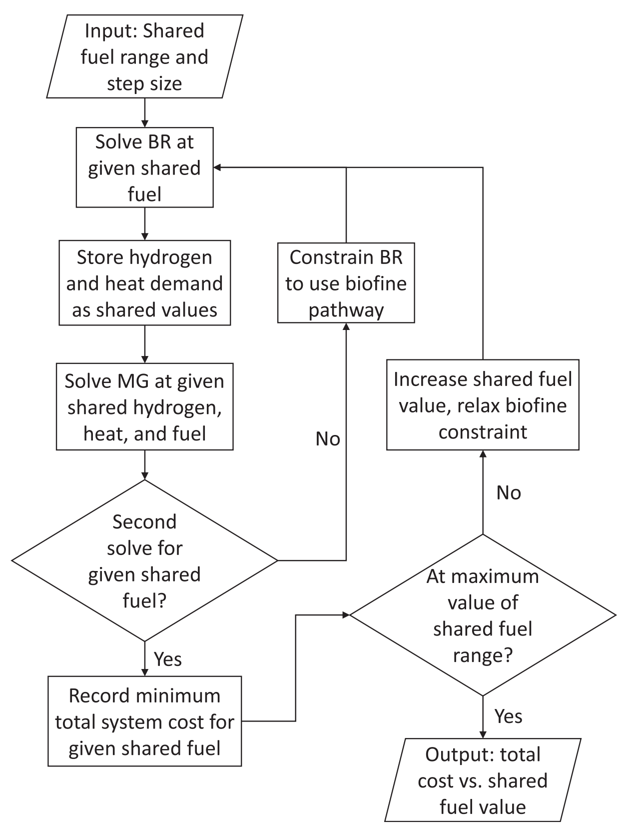

Fig. 4. Algorithm for solving combined optimization problem.

equilibrium terms are relaxed by converting to yield-based equations and using empirically determined upper and lower bounds for the yields. Nonlinear capital cost terms are relaxed using piecewise linear approximations. Binary variables are relaxed to continuous ones with bounds of zero and one. Bounds for McCormick envelopes and equilibrium yields are determined by solving the mass balance for various extreme cases.

3. Case study

The following case study analyzes the cost of implementing the proposed microgrid and biorefinery system in a small community. The microgrid is constrained to meet the power and heat demands of a town consisting of 100 residential homes, a primary and secondary school, a supermarket, and an outpatient center. Data used is that from a typical meteorological year in Minneapolis, MN [33]. The biorefinery is constrained to meet 0.1% of the average hourly liquid fuel demand in the state of Minnesota [40]. As a first step, supply and demand data is assumed to be deterministic, and no uncertainty in the data is considered.

In the base case, the cost of optimizing the systems individually is compared with the cost of optimizing the combined systems. For individual operation, separate cases where the microgrid is and is not allowed to purchase fuel from the centralized infrastructure are considered. Allowing fuel purchasing will present the lowest cost system, while disallowing it mirrors a more distributed system that is not reliant on the centralized infrastructure, presenting a more even comparison with the combined system. Cases where excess hydrogen in the biorefinery is recycled and where the communities are less than 100% reliant on obtaining energy from the new system are also considered.

3.1. Base case

For the base case, the biorefinery NLP and microgrid MILP were solved individually to a 0.1% optimality gap for two cases: where microgrid fuel purchasing is allowed and where it is forbidden. The biorefinery pathway chosen is shown in Fig. 5, and optimization results are summarized in Table 6. Of note when comparing the two individual system problems is that when allowed to purchase fuel, the optimization does not select any hydrogen storage, instead opting to purchase fuel when needed to offset the lack of renewables. Both solutions install wind capacity, but an order of magnitude capacity higher is required when not purchasing fuel. This is due to the intermittancy of wind energy; wind needs to overproduce energy when it is available to compensate for when it is not, absent any other energy source.

The combined system optimal design is found using the algorithm described in section 2.3. Fig. 6 shows the optimal system cost as a function of shared fuel between the two systems. For the combined system, a different biorefinery pathway is selected, depicted in Fig. 7. This pathway is used to limit the hydrogen and heat requirements of the gasifier pathway, which are higher than the biofine pathways. This reduces the cost of the microgrid subsystem. The importance of selecting the biofine pathway when combining the two systems is seen in comparing the cost: if only gasification were used, the cost of the combined system would be $907.026MM, almost double the optimal cost found. This is in spite of the fact that individually, the biorefinery without biofine hydrolysis is less expensive, and demonstrates an effect of the synergies between the two systems.

Despite the aforementioned synergies, the combined system costs are greater than the total costs of the individual systems in both cases considered. This increase in cost comes almost solely from an increase in microgrid costs. The wind and microturbine capacity are about double their individual system value. There are also increases in heater and electrolyzer size. However, the fuel cell is an order of magnitude smaller than in the individual systems case without fuel purchasing despite the larger electolyzer size. Thus, a majority of the hydrogen produced is used to meet continuous hydrogen demand of the biorefinery instead of being stored for future energy needs. To meet this continuous demand, the electrolyzer must run for a longer period of time than it would in the individual systems case. This fact is a primary cause for the high costs of the combined system and motivates further study on the hydrogen system, which is discussed in section 3.3.

Note that in all three cases presented in Table 6, no solar energy is installed in the optimal design. This makes sense considering that solar energy is not prevalent in Minnesota, particularly in the winter when the days are very short. Additionally, wood chips are chosen as the optimal biomass feedstock in all three cases. This is because, despite having a higher cost than wheat straw and corn stover, wood has much less ash and thus more usable carbon than the other feedstocks, making it less expensive on a per carbon basis.

3.2. Utility cost sensitivity cases

One of the advantages of a combined system is that all utilities are provided for within the system; the only material which must be continuously purchased is biomass feedstock. As such, the combined system cost will not be sensitive to uncertainties and changes in utility costs. However, the individual systems' costs will be dependent on these uncertainties. Due to this, it is apparent that after some increase in utility costs, the individual systems' costs will be greater than that of the combined system. This is analyzed by increasing the costs of heat, hydrogen, and fuel from their base case values. The results of this analysis show that individual and combined system costs are equal after a 750% and 500% increase in utility costs for the cases with and without fuel purchasing, respectively. Fig. 8 displays utility cost increases from the base case versus system cost. These results show that it is unreasonable to expect utility cost increases that make the combined system

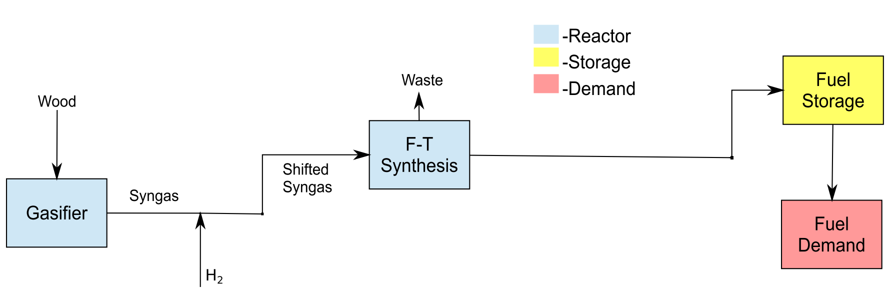

Fig. 5. Optimal biorefinery pathway for separately optimized system.

Table 6
Results of base case optimization for separate and combined systems.

	Individual Systems		Combined System
	Fuel Purchasing	No Fuel Purchasing	
Biomass feed	Wood	Wood	Wood
Feedstock Flowrate (kg/h)	6342	6342	7358
Biofine hydrolysis used?	No	No	Yes
Fischer–Tropsch used?	Yes	Yes	Yes
Wind capacity (MW)	1.8	51.2	109.5
Microturbines capacity (MW)	2.83	0	6.23
Fuel cell capacity (MW)	0	8.15	0.47
Electric heater capacity (MW)	2.19	7.86	14.03
Electrolyzer capacity (kg/hr H_2)	0	516	803
Microgrid average fuel demand (gal/h)	78.7	0	208.3
Biorefinery hydrogen demand (kg/h)	275.5	275.5	240.2
Biorefinery heat demand (MW)	7.80	7.80	7.70
Biorefinery Cost (MM$)	150.5	150.5	152.95
Microgrid Cost (MM$)	37.6	209.5	374.9
Capital Cost (MM$)	61.0	246.0	466.2
Operating Cost (MM$)	127.2	113.9	61.7
Total Cost(MMS)	**188.2**	**360.0**	**527.9**
Cost Lower Bound (MM$)	188.0	359.6	499.7
Optimality Gap(%)	0.1	0.1	5.6

The bold in table is used to emphasize the total costs for each case.

cheaper than the individual systems. Instead, improvements in the combined system are necessary to achieve desired economics.

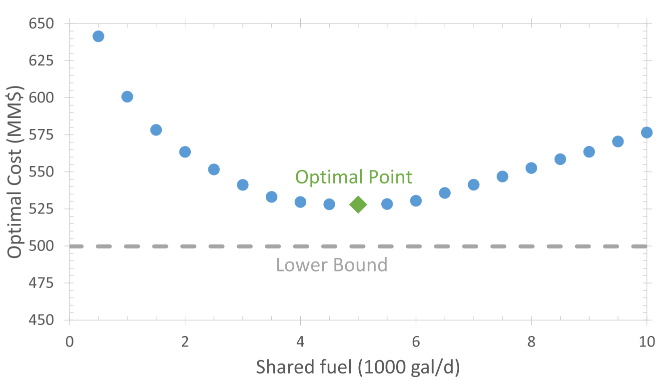

Fig. 6. Optimal system cost as a function of shared fuel for base case combined system.

3.3. Hydrogen recycle cases

Motivated by the base case results, a pressure swing absorption (PSA) unit was added to the biorefinery to recover and recycle some of the excess hydrogen outputted from the biorefinery. To implement this into the model, an additional capital cost term was added to the objective function. The PSA unit had a reference cost of $28 MM for a reference capacity of 100,000 kg H_2/day, and a capacity exponent of 0.75 [41]. Also, the amount of hydrogen bought or demanded from the microgrid was modified as follows:

$$H = \sum_{i \in H_2 \text{ feeds}} \dot{m}_i - \rho \sum_{i \in H_2 \text{ outputs}} x_{i,H_2} \dot{m}_i \tag{40}$$

Note that this reduces to the simpler hydrogen usage equation when ρ=0. The cases of 90% (an upper bound on the capabilities of the PSA unit) and 75% of hydrogen being recycled (a more reasonable value) are analyzed.

When implementing the hydrogen recycle, little change is seen when optimizing the systems individually. The biorefinery sees an extra $3MM in capital cost due to the addition of the PSA unit and an operating cost reduction of $21MM and $25MM for 75% and 90%

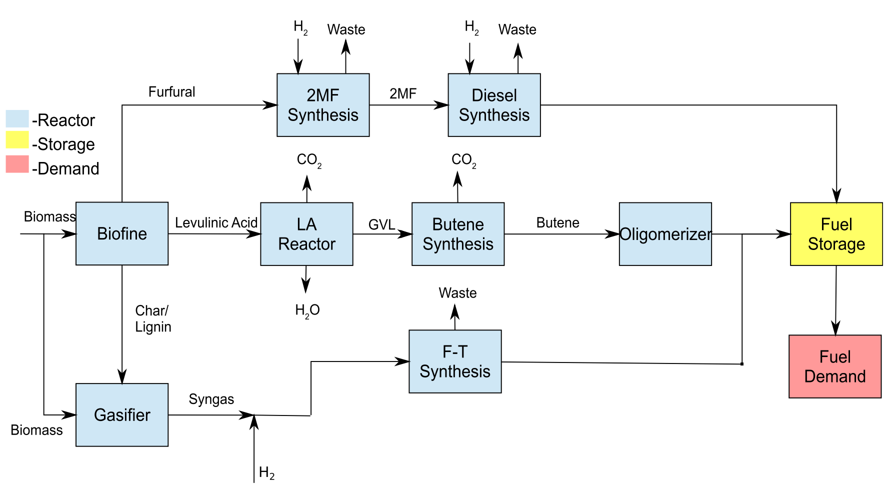

Fig. 7. Base case optimal biorefinery pathway for combined system.

Please cite this article in press as: A. Allman, P. Daoutidis, Optimal design of synergistic distributed renewable fuel and power systems, Renewable Energy (2016), http://dx.doi.org/10.1016/j.renene.2016.03.051

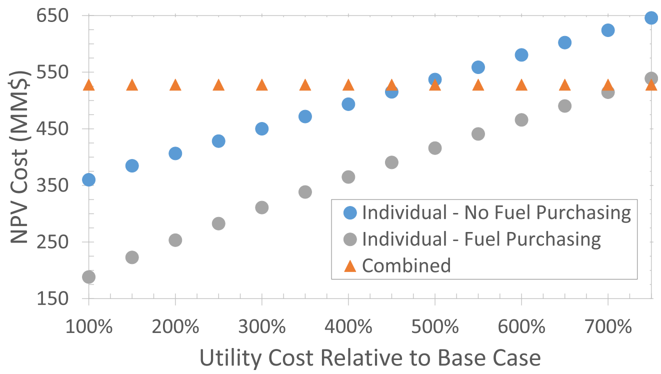

Fig. 8. Utility cost increase vs. system cost for individual and combined systems.

recycle, respectively, due to less hydrogen purchasing. In the 90% recycle case, more hydrogen is recycled than is needed by the biorefinery since hydrogen is a by-product of the water–gas shift reaction which occurs in the Fischer–Tropsch reactor. Thus, in this case, the extra hydrogen is sold for a credit. No change is seen in the microgrid for the individually optimized system since no equations for that system are altered. Feeds, unit sizes, and chosen biorefinery technologies are the same as in the base case individual systems.

When considering the combined system, significant cost reduction is observed. For 75% recycle, a cost reduction of 37% occurs to reduce the NPV cost to $333.7MM. This is in spite of the biorefinery costs increasing from $153.0MM with no recycle to $187.2MM with 75% recycle. Because of the hydrogen recycle, the biorefinery can operate at a higher capacity to share more fuel with the microgrid without stressing the microgrid with high hydrogen demand. The result is a lower overall cost.

Although significant cost reduction is observed with a hydrogen recycle, the combined system is still more expensive than the individual systems in the case where fuel is purchased. This, however, is unsurprising since the biorefinery technology considered cannot yet compete in terms of price with petroleum-based fuels. However, the savings from hydrogen recycle makes the combined system cheaper than the individual systems without fuel purchasing. Further cost reduction is seen in the 90% recycle case. The combined system with recycle still selects the biofine pathway for the biorefinery, and because of this, excess hydrogen is not produced in the reactor as is seen in the individual systems case. Note that no fuel cell is built in the combined systems case with recycle, which indicates that it is more cost-effective to provide energy with fuel from the biorefinery than from stored hydrogen when renewable availability is low. A summary of the combined system results, as well as the individual systems results with no fuel purchasing, with recycle is shown in Table 7.

Further analysis focused on finding the critical recycle ratio where the cost of the combined and individual systems are equal. Linear interpolation was used to predict the point where the costs become equal. Individual and combined system optimization problems were solved and the process was repeated until convergence within $1MM. When doing so, it is seen that the NPV cost of the individual systems without fuel purchasing and the combined systems are equal at 70.9%. In Fig. 9, the recycle ratio vs. cost for the three systems considered is shown. While the combined case cannot compete with the individual case where fuel purchasing is allowed, at recycle rates above 70.9% it is the superior system among the two considered that operate mostly independently from the centralized infrastructure.

Table 7
Results of optimization for recycle cases for separately optimized systems without fuel purchasing and for combined systems.

	Individual Systems		Combined System	
Recycle Ratio	75%	90%	75%	90%
Biomass feed	Wood	Wood	Wood	Wood
Feedstock Flowrate (kg/h)	6343	6346	9554	9279
Biofine hydrolysis used?	No	No	Yes	Yes
Fischer–Tropsch used?	No	No	No	No
Wind capacity (MW)	51.2	51.2	38.1	29.4
Microturbines capacity (MW)	0	0	6.05	5.85
Fuel cell capacity (MW)	8.15	8.15	0	0
Electric heater capacity (MW)	7.86	7.86	15.92	15.28
Electrolyzer capacity (kg/hr H_2)	516	516	280	217
Microgrid average fuel demand (gal/h)	0	0	375.0	354.2
Biorefinery hydrogen demand (kg/h)	40.8	−6.2	114.0	72.3
Biorefinery heat demand (MW)	7.80	7.81	9.99	9.71
Biorefinery Cost (MM$)	132.9	129.2	187.2	183.7
Microgrid Cost (MM$)	209.5	209.5	146.5	118.0
Capital Cost (MM$)	249.3	249.8	217.4	242.4
Operating Cost (MM$)	93.0	88.9	62.4	59.2
Total cost(MM$)	**342.3**	**338.7**	**333.7**	**301.7**
Cost Lower Bound (MM$)	342.0	338.4	293.0	270.5
Optimality Gap(%)	0.1	0.1	14.7	11.5

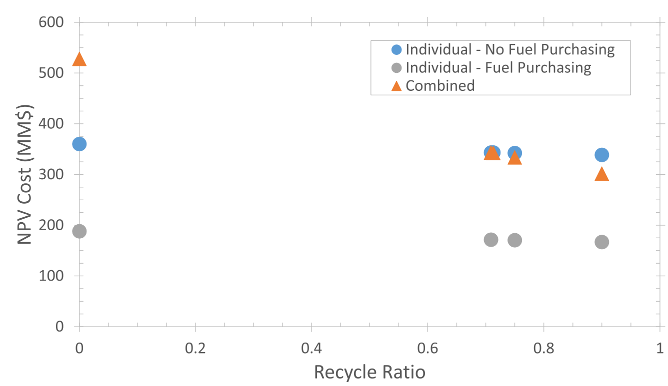

Fig. 9. Recycle ratio vs. cost for individual and combined systems.

3.4. Varying autonomy cases

The previous cases presented all considered operation where the end users are only reliant on the microgrid and biorefinery for energy demand. This 100% autonomy scenario may be ideal for a truly distributed infrastructure, but in practice, some interaction with the macrogrid and global fuel market is to be expected. As such, it is instructive to examine the effect of autonomy on the individual and combined systems. To analyze these effects, the following changes are made to the heat, power, and fuel demand equations:

$$\sum_{j \in \text{heat out}} \dot{e}_{j,t} \geq \omega(\delta_{h,t} + Q) \ \forall t \tag{41}$$

$$\sum_{j \in \text{power out}} \dot{e}_{j,t} = \omega \delta_{p,t} \ \forall t \tag{42}$$

$$\sum_{i \in \text{fuel outputs}} \dot{m}_i = \omega\left(\delta_f + F\right) \tag{43}$$

Note that equations (41–43) reduce to the simpler demand equations when $\omega = 1$. When considering autonomy of less than 100%, the balance of fuel, power, and heat demand that is not met by the system is assumed to be purchased at its market value. The objective function is modified to match this change.

When analyzing how autonomy affects the cost of the individual systems, it is seen that increasing the autonomy does not make the combined system perform better when not considering recycle. In fact, the place where the cost of the combined system and individual systems meet is at 0% autonomy, or the case where nothing is built and all fuel and power is obtained from the centralized infrastructure. In the intermediate range of autonomy levels, the unit sizes are simply scaled down to match the lower demand on the biorefinery and microgrid system. A more interesting case occurs when hydrogen recycle is considered. By finding the critical recycle ratio as a function of autonomy, further evidence of synergies between the biorefinery and microgrid are apparent. This relationship is plotted in Fig. 10. The general trend is that the critical recycle ratio decreases as autonomy decreases, although there is a slight upward kink at 25% autonomy. This means that, in general, as the connections with the centralized infrastructure improve and/or the load serviced by the biorefinery and microgrid decreases, a combined system becomes even more cost competitive with the individual systems. These results show that although combining the systems was motivated by a desire for greater resiliency, a combined system can also be desirable when connections to the centralized infrastructure do exist.

4. Conclusions and future work

This paper presented a framework for the design optimization of a combined microgrid and biorefinery system. While the resulting large MINLP is much more difficult to solve than its constituent parts, the natural structure of the combined system was exploited to make the problem tractable through a primal decomposition approach. This decomposition was applied to a base case that showed that the optimal combined system cost of $527.9MM was much higher than the total cost of the individually optimized systems. However, a direct effect of synergy between the two systems was seen in this base case, as the optimal biorefinery pathway found in the combined system was different than that found in the individually optimized system.

Further analysis of the combined biorefinery and microgrid system examined other effects of synergy. The implementation of a hydrogen recycle using a PSA unit showed a simple way to make a combined biorefinery and microgrid system cost-competitive with the individually optimized systems. Cost reduction from hydrogen recycle is a direct result of system synergy: implementing a 75% recycle reduces combined system costs by 37%, as opposed to just 5% reduction in the individual systems. The autonomy analysis shows that a combined system can also be competitive and desirable even when connection to the centralized infrastructure is considered.

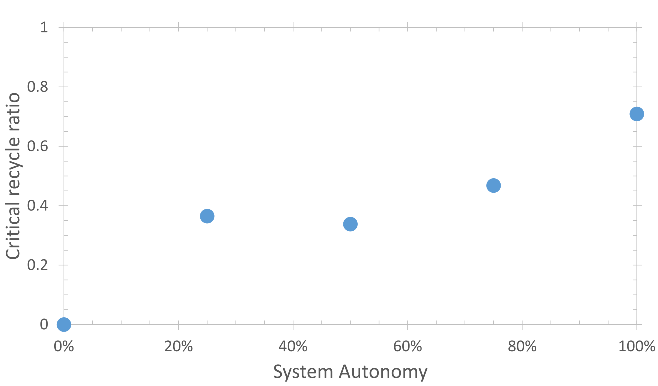

Fig. 10. Critical recycle ratio vs. system autonomy.

The proposed power and fuel polygeneration system is a meaningful example of a system of systems, physically coupled systems with different functionalities but also linked through a common managing entity. The potential beneficial synergies in such systems can be significant, but so are the resulting challenges in design and operation. The present study is just a first step the development of efficient design and control methods for such synergistic renewable fuel and power systems. Future research will examine the effects of uncertainty in renewable availability and energy demand on the design of such systems, as well as the corresponding scheduling and control problems.

Acknowledgments

Funding for this project was provided in part by the Minnesota Environment and Natural Resoures Trust Fund as recommended by the Legislative-Citizen Commission on Minnesota Resources (LCCMR). Financial support from the MnDRIVE transdisciplinary research award is also gratefully acknowledged.

References

[1] R.H. Lasseter, Micrograds and distributed generation, J. Energy Eng. 133 (2007) 144–149.
[2] H.L. Wakeley, C.T. Hendrickson, W.M. Griffin, H.S. Matthews, Economic and environmental transportation effects of large-scale ethanol production and distribution in the United States, Environ. Sci. Technol. 43 (2009) 2228–2233.
[3] B. Antizar-Ladislao, J.L. Turrion-Gomez, Second-generation biofuels and local bioenergy systems, Biofuels Bioprod. Biorefining 2 (2008) 455–469.
[4] A. Kashefi Kaviani, G.H. Riahy, S.H.M. Kouhsari, Optimal design of a reliable hydrogen-based stand-alone wind/PV generating system, considering component outages, Renew. Energy 34 (2009) 2380–2390.
[5] R. Dofo-Lopez, J.L. Bernal-Agustin, Multi-objective design of PV-wind-diesel-hydrogen-battery systems, Renew. Energy 33 (2008) 2559–2572.
[6] O. Hafez, K. Bhattacharya, Optimal planning and design of a renewable energy based supply system for microgrids, Renew. Energy 45 (2012) 7–15.
[7] M. Zachar, P. Daoutidis, Understanding and predicting the impact of location and load on microgrid design, Energy 90 (2015) 1005–1023.
[8] H. Li, H. Hong, H. Jin, R. Cai, Analysis of a feasible polygeneration system for power and methanol production taking natural gas and biomass as materials, Appl. Energy 87 (2010) 2846–2853.
[9] P. Liu, E.N. Pistikopoulos, Z. Li, A multi-objective optimization approach to polygeneration energy systems design, AIChE J. 56 (2010) 1218–1234.
[10] A. Kelloway, P. Daoutidis, Process synthesis of biorefineries: optimization of biomass conversion to fuels and chemicals, Ind. Eng. Chem. Res. 53 (2013) 5261–5273.
[11] R.C. Baliban, J.A. Elia, C.A. Floudas, Toward novel hybrid biomass, coal, and natural gas processes for satisfying current transportation fuel demands, 1: process alternatives, gasification modeling, process simulation, and economic analysis, Ind. Eng. Chem. Res. 49 (2010) 7343–7370.
[12] R.C. Baliban, J.A. Elia, C.A. Floudas, Biomass to liquid transportation fuels (BTL) systems: process synthesis and global optimization framework, Energy Environ. Sci. 6 (2013) 267–287.
[13] D.K.S. Ng, Automated targeting for the synthesis of an integrated biorefinery, Chem. Eng. J. 162 (2010) 67–74.
[14] V. Pham, M. El-Halwagi, Process synthesis and optimization of biorefinery configurations, AIChE J. 58 (2012) 1212–1221.
[15] B. Wang, B.H. Gebrelassie, F. You, Sustainable design and synthesis of hydrocarbon biorefinery via gasification pathway: integrated life cycle assessment and technoeconomic analysis with multiobjective superstructure optimization, Comput. Chem. Eng. 52 (2013) 55–76.
[16] D.J. Hayes, S. Fitzpatrick, M.H. Hayes, J.R. Ross, The biofine process – production of levulinic acid, furfural, and formic acid from lignocellulosic feedstocks, in: B. Kamm, P.R. Gruber, M. Kamm (Eds.), Biorefineries – Industrial Processes and Products: Status Quo and Future Directions, WILE-VCH Verlag GmbH & Co. KGaA, Weinheim, Germany, 2008, pp. 139–164.
[17] S. Murat Sen, C.A. Henao, D.J. Braden, J.A. Dumesic, C.T. Maravelias, Catalytic conversion of lignocellulosic biomass to fuels: process development and technoeconomic conversion, Chem. Eng. Sci. 67 (2012) 57–67.
[18] A. Corma, O. de la Torre, M. Renz, N. Villandier, Production of high-quality diesel fuel from biomass waste products, Angew. Chem. 123 (2011) 2423–2426.
[19] P. Spath, A. Aden, T. Eggeman, M. Ringer, B. Wallace, J. Jechura, Biomass to Hydrogen Production Detailed Design and Economics Utilizing the Battelle Columbus Laboratory Indirectly-Heated Gasifier, 2005. Technical report.

[20] J. Douglas, Conceptual Design of Chemical Processes, McGraw Hill, New York, 1988.
[21] J. Kuo, Slurry Fischer-Tropsch/Mobil Two Stage Process of Converting Syngas to High Octane Gasoline, 1983. Final report.
[22] S.D. Phillips, J.K. Tarud, M.J. Biddy, A. Dutta, Gasoline From Wood via Integrated Gasification, Synthesis, and Methanol to Gasoline Technologies, 2011. Technical report.
[23] U.S. Department of Energy, Biomass feedstock composition and property database (2004). URL http://www.afdc.energy.gov/biomass/progs/search1.cgi.
[24] R.W. Zwart, H. Boerrigter, High efficiency cogeneration of synthetic natural gas (SNG) and Fischer–Tropsch (FT) transportation fuels from biomass, Energy Fuels 19 (2005) 591–597.
[25] C.E. Harvie, J.P. Greenberg, J.H. Weare, A chemical equilibrium algorithm for highly non-ideal multiphase systems: free energy minimization, Geochim. Cosmochim. Acta 51 (1987) 1045–1057.
[26] National Institute of Standards and Technology, NIST chemistry webbook (2011). URL http://webbook.nist.gov.
[27] M. Tawarmalani, N.V. Sahinidis, A polyhedral branch-and-cut approach to global optimization, Math. Program. 103 (2005) 225–249.
[28] M. Zachar, M. Trifkovic, P. Daoutidis, Policy effects on microgrid economics, technology selection, and environmental impact, Comput. Chem. Eng. 81 (2015) 365–375.
[29] R. Wiser, M. Bollinger, G. Barbose, K. Belyeu, M. Hand, D. Heimiller, D. Lew, M. Milligan, A. Mills, A. Moreno, W. Musial, R. O'Connell, K. Porter, Z. Subin, Annual Report on U.S. Wind Power Instillation, Cost, and Performance Trends: 2006, 2008. Technical report.
[30] National Renewable Energy Laboratory, The open PV project (2015). URL https://openpv.nrel.gov/index.
[31] G. Saur, T. Ramsden, Wind Electrolysis: Hydrogen Cost Optimization, 2011. Technical report.
[32] Breakthrough Technologies Institute, Inc, 2011 Fuel Cell Technologies Market Report, 2012. Technical report.
[33] U.S. Department of Energy, Commercial and residential hourly load profiles fo all TMY3 locations in the united states (2013). URL http://en.openei.org/datasets/dataset/commercial-and-residential-hourly-load-profiles-for-all-tmy3-locations-in-the-united-states.
[34] M.A. Green, K. Emery, Y. Hishikawa, W. Warta, E.D. Dunlop, Solar cell efficiency tables, Prog. Photovolt. Res. Appl. 22 (2014) 701–710.
[35] M. Carmo, D.L. Fritz, J. Mergel, D. Stolten, A comprehensive review on PEM water electrolysis, Int. J. Hydrog. Energy 38 (2013) 4901–4934.
[36] R. Barbir, T. Gomez, Efficiency and economics of proton exchange membrane (PEM) fuel cells, Int. J. Hydrog. Energy 22 (1997) 1027–1037.
[37] S. Lee, I.E. Grossmann, New algorithms for nonlinear generalized disjunctive programming, Comput. Chem. Eng. 24 (2000) 2125–2141.
[38] L.S. Lasdon, Optimization Theory for Large Systems, Courier Corporation, Mineola, NY, 2013.
[39] P.M. Pardalos, H.E. Romeijn (Eds.), Handbook of Global Optimization, vol. 2, Springer Science+Business Media, Dordrecht, Netherlands, 2002.
[40] Minnesota Department of Commerce, Fuel Monitoring Reports This Week, 2014. Technical report.
[41] D. Simbeck, E. Chang, Hydrogen Supply: Cost Estimate for Hydrogen Pathways – Scoping Analysis, 2002. Technical report.

Please cite this article in press as: A. Allman, P. Daoutidis, Optimal design of synergistic distributed renewable fuel and power systems, Renewable Energy (2016), http://dx.doi.org/10.1016/j.renene.2016.03.051